

Published in final edited form as:

*J Neurochem.* 2010 May ; 113(4): 943–951. doi:10.1111/j.1471-4159.2010.06657.x.

## Quantal release of acetylcholine in mice with reduced levels of the vesicular acetylcholine transporter

Ricardo de Freitas Lima<sup>1</sup>, Vania F. Prado<sup>2</sup>, Marco A. M. Prado<sup>2</sup>, and Christopher Kushmerick<sup>1</sup>

<sup>1</sup> Departamento de Fisiologia e Biofísica, Instituto de Ciências Biológicas, Universidade Federal de Minas Gerais, 31270-901 Minas Gerais, Brasil.

<sup>2</sup> Molecular Brain Research Group, Robarts Research Institute, Department of Physiology and Pharmacology and Department of Anatomy and Cell Biology, University of Western Ontario

### Abstract

Mammalian motor nerve terminals contain hundreds of thousands of synaptic vesicles, but only a fraction of these vesicles is immediately available for release, the remainder forming a reserve pool. The supply of vesicles is replenished through endocytosis, and newly formed vesicles are refilled with acetylcholine through a process that depends on the vesicular acetylcholine transporter (VACHT). During expression of short-term plasticity, quantal release can be increased, but it is unknown whether this reflects enhanced recruitment of vesicles from the reserve pool or rapid recycling. We examined spontaneous and evoked release of acetylcholine at endplates from genetically modified VACHT KD<sup>HOM</sup> mice that express approximately 30% of the normal level of VACHT in order to determine steps rate-limited by synaptic vesicle filling. Quantal content and quantal size were reduced in VACHT KD<sup>HOM</sup> mice compared to wild-type controls. Although high-frequency stimulation did not reduce quantal size further, the post-tetanic increase in EPP amplitude or MEPP frequency was significantly smaller in VACHT KD<sup>HOM</sup> mice. This was the case even when tetanic depression was eliminated using an extracellular solution containing reduced Ca<sup>2+</sup> and raised Mg<sup>2+</sup>. These results reveal the dependence of short-term plasticity on the level of VACHT expression and efficient synaptic vesicle filling.

### Keywords

acetylcholine; neuromuscular junction; quantal content; MEPP; transport; post-tetanic potentiation; synaptic vesicle

### Introduction

Neurotransmission at chemical synapses is initiated by an action potential in the pre-synaptic nerve terminal that opens Ca<sup>2+</sup> channels and triggers exocytosis of neurotransmitter. The post-synaptic impact of each event depends on the number of quanta released, the amount of neurotransmitter per quanta, and the post-synaptic sensitivity. All three of these factors, and thus the overall efficiency of neurotransmission, depend on the recent firing activity of the neurons involved, a phenomenon referred to as synaptic short-term plasticity (Zucker and Regehr, 2002). Different forms of short-term plasticity are recognized based on the pattern of activity required for their generation and the

characteristic time course of their decay. At the frog neuromuscular junction short-term increases in neurotransmitter release have been classified as facilitation, augmentation, and potentiation (Magleby and Zengel, 1982). Facilitation can be generated by a single conditioning stimulus and decays with a time constant of less than 1 sec. In contrast, augmentation and post-tetanic potentiation follow repetitive stimulation and last for seconds or minutes, respectively. Qualitatively similar phenomena have been described at the mammalian neuromuscular junction (Gage and Hubbard, 1966; Bain and Quastel, 1992), autonomic synapses (Zengel et al., 1980), as well as many central synapses (Zucker, 1989; Fisher et al., 1997).

Potentiation of EPP amplitude could be caused by an increase in size of the quanta or an increase in the number of quanta that make up each EPP. At the frog neuromuscular junction, repetitive stimulation did not alter quantal size measured as the MEPP amplitude (Zengel and Sosa, 1994). Later measurements of MEPC charge integrals indicated a reduction in the amount of acetylcholine per quanta after repetitive stimulation (Naves and Van der Kloot, 2001). Since quantal size evidently is not increased by tetanic stimulation, this leaves an increase in quantal content as the likely cause of EPP potentiation. Quantal content reflects release probability ( $P$ ) and number of release sites or vesicles ( $N$ ) both of which change during a conditioning train and in the post-tetanic period. The vertebrate motor nerve terminal contains a large number of synaptic vesicles, but at a given moment, only a small fraction participate in evoked neurotransmitter release, the remainder comprising a reserve pool (Rizzoli and Betz, 2005). It is therefore evident that during periods of increased release, vesicle recycling or recruitment from the reserve pool must be augmented to avoid depletion of release-ready synaptic vesicles.

There are many steps in the pathways that prepare synaptic vesicles for release and subsequently recycle them for reuse (Sudhof, 2004). Active transport of acetylcholine into cholinergic vesicles is mediated by the vesicular acetylcholine transporter (VACHT) (Erickson et al., 1994; Roghani et al., 1994). Previous experiments demonstrate accelerated depression of synaptic currents and loss of quantal size when nerve terminals are stimulated in the presence of vesamicol, an inhibitor of VACHT (Searl et al., 1991; Prior et al., 1992). Vesicle filling by VACHT represents an essential step for neuromuscular function, as genetically altered VACHT  $KD^{HOM}$  mice with reduced expression of VACHT are myasthenic (Prado et al., 2006) and VACHT knock-out mice are not viable due to a lack of neuromuscular function (de Castro et al., 2009).

In the present work, we tested the consequence of reduced VACHT on quantal size and quantal content at rest and after tetanic stimulation in neuromuscular junctions from VACHT  $KD^{HOM}$  mice that express approximately 30% of the normal levels of VACHT to investigate how deficits in vesicular transport affect quantal release of acetylcholine.

## Methods

### Animals

Generation of VACHT  $KD^{HOM}$  mice has been described in detail (Prado et al., 2006). Animals were housed in groups of 3-5 mice/cage in a temperature-controlled room with a 12:12 light:dark cycles and food and water were provided ad libitum. All studies were performed in accordance with protocols approved by the local institutional animal use and welfare committee (CETEA-UFGM protocol 073/03) and followed the NIH guidelines for care and use of animals in research. Experiments were performed "blind" in the sense that the genotype of the animal was unknown until all experiments and analysis were complete.

## Isolation of hemi-diaphragm

Mice were killed by decapitation and the diaphragm with attached nerve rapidly removed and pinned in an acrylic chamber on a bed of silicone elastomer (Sylguard). The preparation was continuously perfused at a rate of 2-3 ml/min with physiological solution containing (in mM): NaCl (137), NaHCO<sub>3</sub> (26), KCl (5), NaH<sub>2</sub>PO<sub>4</sub> (1.2) glucose (10), CaCl<sub>2</sub> (2.4), and MgCl<sub>2</sub> (1.3), pH adjusted to 7.4 after gassing with 95% O<sub>2</sub> / 5% CO<sub>2</sub>. In some experiments quantal content was reduced by changing the concentrations of CaCl<sub>2</sub> and MgCl<sub>2</sub> as described in the Results. Experiments were conducted at room temperature (22-24°C). To avoid muscle contraction during nerve stimulation (+)-tubocurarine (curare, 0.8-2.9 microM, Sigma-Aldrich) was included in the bath or the muscle fibers were cut (Barstad and Lilleheil, 1968). Salts were purchased from Sigma-Aldrich or Vetec Quimica Fina (Rio de Janeiro).

## Electrophysiology

Recordings were made using an Axoclamp-2A 10X preamplifier. Microelectrodes were fabricated from borosilicate glass (WPI, 1B150F-4) using a Narishige PN-30 puller and had resistances of 8-15 MΩ when filled with 3 M KCl. Microelectrodes were inserted into the muscle fiber near the end-plate region as judged by the presence of MEPPs with rise times < 1ms. Signals were band-pass filtered at 0.1-5 KHz and further amplified 10-100x as necessary. In addition, the DC membrane potential was recorded for correction of driving force and non-linear summation of EPPs. Data were acquired on a PC computer equipped with a National Instruments A/D board and running Strathclyde Electrophysiology Software (kindly provided by John Dempster, University of Strathclyde). MEPP and EPP amplitudes were corrected to a standard resting potential of -60mV or -35mV when the cut-fiber technique was used and corrected for non-linear summation when EPP amplitude exceeded 10% of the driving force assuming a reversal potential of 0 mV for synaptic current (McLachlan and Martin, 1981).

For stimulation, the nerve was drawn into a suction electrode and stimulated with suprathreshold voltage pulses (0.1 ms duration). Contractions were blocked by submaximal concentrations of d-tubocurarine (curare, 0.8-2.9 microM, Sigma-Aldrich), or by recording in a low-Ca<sup>2+</sup> / high-Mg<sup>2+</sup> bathing solution containing 0.6 mM Ca<sup>2+</sup> and 7 mM Mg<sup>2+</sup>, or by cutting the muscle fibers (Barstad and Lilleheil, 1968). Facilitation was evaluated using paired pulses (10 ms inter pulse interval) applied at 0.1 Hz. Stimulus trains consisting of 200-3000 stimuli delivered at 30-50 Hz were used to study augmentation and post-tetanic potentiation. When more than one NMJ was evaluated in the same muscle, the minimum interval between stimulus trains was 10 min which was sufficient for full recovery. Quantal content was calculated by the direct method as (EPP/MEPP) where the average MEPP amplitude was calculated as the mean of at least 40 MEPPs (usually >50). Coefficient of variation of EPP amplitudes was determined from 20 EPPs evoked at 0.5 Hz. In recordings using very low-Ca<sup>2+</sup> / high-Mg<sup>2+</sup> Tyrodes solution quantal content was <1 and permitted measurement of quantal content by the statistical methods of Del-Castillo and Katz, (1954) with minor modifications. We applied stimuli once per second. EPPs were recorded following each stimuli, and MEPPs were captured during the period between stimuli, excluding the 40 ms that followed the stimulus. We measured  $F_{failure}$ , the fraction of stimuli not followed by an EPP, and calculated quantal content as  $-\ln(F_{failure})$  (Martin, 1966). We used this estimate of quantal content and the quantal size of the MEPPs measured at the same synapse to fit the observed EPP distributions with no free parameters. With the same data, we calculated quantal content by the direct method for comparison.

## Analysis

MEPPs were detected in the intracellular recordings using the template search algorithm in Clampfit 9.2 (Axon Instruments). The template was constructed by averaging 3 or 4 MEPPs identified by eye. All MEPPs identified by the program were inspected, and the Template Match Threshold parameter was adjusted to minimize false positives. Data were exported from Clampfit and analysed using custom macros written in Igor software (Wavemetrics, Lake Oswigo, Or, USA).

Data are presented as mean  $\pm$  95% confidence intervals. The 95% confidence intervals were calculated assuming a Student's t distribution in the means. All results were means from between three and six (usually four) animals of each genotype. In each nerve-muscle preparation, between one and five (usually three) endplates were studied. Sample sizes used to calculate 95% confidence intervals were the number of endplates studied. Where appropriate, data were analyzed either by unpaired Student's t-test or one-way ANOVA followed by Tukey's post hoc test.

## Results

### Quantal parameters during low-frequency stimulation

To examine effects of reduced VAcHT expression on quantal acetylcholine release, we measured end-plate potentials (EPPs) in diaphragm neuromuscular junctions from wild-type and VAcHT KD<sup>HOM</sup> mice. A low frequency of stimulation was used (0.5 Hz) which generated little synaptic plasticity. In an extracellular solution containing 1.2 mM Ca<sup>2+</sup> and 1.3 mM Mg<sup>2+</sup>, evoked EPPs recorded from VAcHT KD<sup>HOM</sup> animals were smaller than EPPs recorded from their age-matched wild-type controls (Fig. 1). Using the cut-fiber technique to avoid muscle contraction, wild-type EPPs averaged 11.9 $\pm$ 3.5 mV (95% confidence interval) whereas VAcHT KD<sup>HOM</sup> EPPs were 5.5  $\pm$  2.0 mV ( $p < 0.05$ ). To avoid possible artifacts resulting from the muscle fiber depolarization that occurs with the cut-fiber technique, we also measured EPP amplitudes when muscle contraction was blocked with 2.4 microM D-tubocurarine (curare). The use of curare has the additional benefit of reducing EPP amplitudes sufficiently so that that correction for non-linear summation was unnecessary, thus eliminating possible artifacts due to uncertainty in synaptic current reversal potential (McLachlan and Martin, 1981). In these conditions, EPPs were 1.47 $\pm$ 0.30 mV (95% confidence interval) in wild-type diaphragms and 0.95 $\pm$ 0.15 mV for VAcHT KD<sup>HOM</sup> mice ( $p < 0.05$ ).

The amplitude of the EPP reflects both quantal content, which is the mean number of quanta per EPP, and quantal size, which is the unitary effect of each quantum (Del-Castillo and Katz, 1954). We measured quantal size as the average amplitude of >40 MEPPs from each synapse. The distribution in MEPP amplitudes from one WT and one VAcHT KD<sup>HOM</sup> synapse are shown in Fig 1B. MEPP amplitudes approximated a Gaussian distribution in most cases (smooth curves in Fig 1B). We measured EPPs as the average of 20 responses to nerve stimulation applied at 0.5 Hz. On average, the difference between EPP amplitudes in VAcHT KD<sup>HOM</sup> versus wild-type mice was larger than expected based solely on the difference in quantal size (Fig. 1C).

The coefficient of variation of EPP amplitudes during 0.5 Hz trains was significantly larger in VAcHT KD<sup>HOM</sup> mice (WT: 0.10 $\pm$ 0.028 versus KD 0.18 $\pm$ 0.04, mean $\pm$ 95% confidence intervals,  $P < .05$ ). This is an indication of smaller quantal content in the VAcHT KD<sup>HOM</sup> mice because when the mean number of quanta per EPP is smaller, the relative impact of stochastic variations in the number of quanta released is larger. We measured quantal content by the direct method at each endplate as the ratio of EPP to MEPP amplitude (Martin, 1966), and observed it was markedly reduced in EPPs from VAcHT KD<sup>HOM</sup> mice

(Fig. 1D). Whereas wild-type synapses released  $21.5 \pm 3.8$  quanta per EPP (95% confidence interval), in VACHT KD<sup>HOM</sup> synapses the number was  $12.5 \pm 2.5$  quanta per EPP ( $p < 0.05$ ). We conclude that the reduction of EPP amplitude in VACHT KD<sup>HOM</sup> neuromuscular junctions reflects two factors, a reduction of quantal size and a reduction of quantal content.

The observed reduction in quantal content could reflect a difference in release probability between wild-type and VACHT KD<sup>HOM</sup> synapses. To examine release probability, we measured paired-pulse facilitation with an interval between stimuli of 10 ms (Fig. 2). With an extracellular Mg<sup>2+</sup> concentration of 1.3 mM, facilitation was  $29 \pm 5\%$  (95% confidence interval) in wild-type synapses and  $34 \pm 6\%$  in VACHT KD<sup>HOM</sup> (not significantly different). To increase the sensitivity of this measurement, we raised Mg<sup>2+</sup> to 2.5 mM to reduce release probability. In this case facilitation was increased as expected due to the lower release probability (Mallart and Martin, 1968), but there remained no significant difference in facilitation between wild-type and knock-down synapses ( $41 \pm 6\%$  versus  $44 \pm 8\%$ ), suggesting that basal release probability was similar for the two genotypes.

### Responses to tetanic stimulation

We next examined changes in EPP amplitude during high-frequency stimulation. Muscle contractions were blocked by curare. As shown in Fig. 3A, when the stimulation frequency was increased from 0.3 Hz to 30 Hz, EPP amplitude rapidly fell within the first seconds to about 50% of baseline, and slowly declined further over the course of the 90 s stimulus. Upon return to 0.3 Hz stimulation, EPP amplitudes rapidly recovered. WT synapses exhibited clear post-tetanic potentiation of EPPs that returned to initial values with a time constant of approximately 30 s (Fig. 3A, *black solid line*). In VACHT KD<sup>HOM</sup> synapses, the peak EPP after recovery from tetanic stimulation rarely exceeded its initial value. Nonetheless, it was possible to define a small post-tetanic potentiation in these synapses as an exponential decrease of EPP amplitudes in the 100 s after cessation of tetanic stimulation (Fig. 3A, *gray solid line*) that had a similar time course but was smaller than wild-type ( $p < 0.05$ ).

The peak EPP amplitude following tetanic stimulation likely reflects a balance between augmentation/post-tetanic potentiation and residual tetanic depression (Wilson and Skirboll, 1974) both of which may be affected in VACHT KD<sup>HOM</sup> animals. To distinguish these two forms of short-term plasticity, we varied the amount of depression that occurred during the tetanic stimulation by varying the ratio of Ca<sup>2+</sup> to Mg<sup>2+</sup> concentrations (Ca<sup>2+</sup> / Mg<sup>2+</sup>) in the bathing solution (Fig. 3 B-C). As the ratio decreased, steady-state depression at the end of the train decreased (Fig 3B), presumably because the reduction in release probability produces less vesicle pool depletion (Mallart and Martin, 1968). In all three conditions, post-tetanic potentiation was greater in wild-type synapses than in VACHT KD<sup>HOM</sup> (Fig. 3C,  $p < 0.05$ ).

Following a high-frequency stimulus train, the frequency of MEPPs is transiently increased and decays back to resting levels with a time course similar to that of augmentation/post-tetanic potentiation of EPP amplitudes (Nussinovitch and Rahamimoff, 1988; Bain and Quastel, 1992; Zengel and Sosa, 1994). To determine if post-tetanic potentiation viewed in this way was also altered in the VACHT KD<sup>HOM</sup> animals, we repeated the experiments using the cut-fiber preparation without curare. This allowed us to measure MEPPs before and after the tetanic stimulation. As shown in Fig. 4, tetanic stimulation resulted in a large increase in MEPP frequency lasting approximately 30 s in WT mice. This type of potentiation was dramatically reduced in VACHT KD<sup>HOM</sup> mice compared to wild-type controls ( $240 \pm 125\%$  in wild-type versus  $92 \pm 53\%$  in VACHT KD<sup>HOM</sup>; mean  $\pm$  95% confidence intervals,  $p < 0.05$ ). In both wild-type and VACHT KD<sup>HOM</sup> synapses, MEPP amplitude was unaltered by the tetanic stimulation (Fig 4B).

## Comparison of MEPPs and unquantal EPPs

The comparison between MEPP and EPP amplitudes assumes these two events arise from the same pool of synaptic vesicles. Although this has long been a tenet of quantal analysis, recent evidence in hippocampus has appeared both for and against the existence of separate pools of vesicles underlying spontaneous and evoked release (Sara et al., 2005; Groemer and Klingauf, 2007; Fredj and Burrone, 2009). We therefore examined quantal content in low- $\text{Ca}^{2+}$  / high- $\text{Mg}^{2+}$  bathing solution. These experiments allowed direct comparison between the size of MEPPs and unquantal EPPs, permitted analysis of the distribution of EPP amplitudes, and allowed for quantal content calculations based on the statistical methods of (Del-Castillo and Katz, 1954) versus the direct method (Fig. 5).

Results from a representative WT NMJ are shown in Fig. 5A-D. MEPP amplitude distributions and time integral distributions (“areas”) approximated a Gaussian distribution ( $P > 0.1$ , Kolmogorov-Smirnov test for the vertical distance between two cumulative probability distributions). Fig. 5C shows averaged EPPs recorded at the same synapse on the same time scale as Fig. 5A. Two sets of EPPs were grouped for averaging. The smaller waveform is the average of 182 probable unquantal EPPs and the larger waveform is the average of 60 probable diquantal EPPs. These EPPs were selected by first calculating the mean quantal content as  $-\ln(F_{\text{failure}})$  where  $F_{\text{failure}}$  is the fraction of stimuli that failed to evoke release (Martin, 1966). Events (including failures) were ranked by amplitude, and selected using the predictions of the Poisson distribution with the mean given by the measured mean quantal content. Note that the mean unquantal EPP is essentially identical to the mean MEPP (compare Fig. 5A and 5C), and the mean diquantal EPP has twice the amplitude. We conclude that MEPPs and unquantal EPPs are indistinguishable.

To test the assumption that the EPP reflects the sum of one or more MEPPs, we constructed EPP amplitude and area distributions (Fig. 5D, *solid lines*) and fit them with a model distribution with no free parameters (Fig. 5D, *broken lines*). At each synapse, mean quantal content was measured as  $-\ln(F_{\text{failure}})$ . Then, a set of 10000 simulated EPPs were generated with quantal content given by a Poisson distribution matched to the data. To build up the EPPs, MEPP amplitudes or areas were randomly selected with replacement from the population of MEPPs measured at the same synapse. Based on the agreement of the data and the simulation, we find no evidence for a separate pool of quantal generating MEPPs and EPPs. Similar results were obtained from NMJs from 3 WT animals and 4 VACHT-KD<sup>HOM</sup> animals, except that mean quantal content was lower in the VACHT-KD<sup>HOM</sup> animals. In this set of experiments, MEPP frequency was  $0.42 \pm 0.11 \text{ s}^{-1}$  in WT synapses and  $0.27 \pm 0.08 \text{ s}^{-1}$  in VACHT KD<sup>HOM</sup> ( $P < 0.05$ ).

We next compared quantal content measured by the statistical method of counting failures versus the direct method (EPP/MEPP). If EPPs are built up of quanta from the same pool that generates MEPPs, the two estimates should give the same result. Fig. 5E-F summarizes results from 11 WT synapses obtained from 3 animals and 8 VACHT KD<sup>HOM</sup> synapses obtained from 4 animals. In Fig. 5E, open symbols represent data obtained by considering MEPP and EPP amplitudes whereas the filled symbols considered MEPP and EPP areas. The solid line has unity slope. The mean and 95% confidence limits for the three quantal content estimates (method of counting failures, direct method based on amplitudes, and direct method based on amplitudes) shown in Fig. 5F indicate reduced quantal content in VACHT KD<sup>HOM</sup> mice.

## Discussion

In this paper we report changes in quantal acetylcholine release in VACHT KD<sup>HOM</sup> mice in which brain and spinal cord levels of VACHT (both mRNA and protein) are reduced to 30%

of wild-type levels whereas other cholinergic markers including the synthesizing enzyme ChAT and the high-affinity choline transporter CHT1 are normal. Although these mice are myasthenic (Prado et al, 2006), and have reduced parasympathetic tone (Lara et al, 2010), they are viable and survive to adulthood. Accordingly, at the neuromuscular junction MEPPs are readily detectable and nerve stimulation generates large synchronous EPPs. VACHT KD<sup>HOM</sup> mice thus provide a model to study the effect of steady-state reductions in VACHT, and hence synaptic vesicle filling, on quantal release of acetylcholine, and to test for the dependence of short-term plasticity on efficient synaptic vesicle filling. Previously, we showed enhanced depression of quantal content during very high-frequency stimulation (100 Hz) and 2.4 mM Ca<sup>2+</sup> to enhance quantal output (Prado et al., 2006). Here, we used lower frequency stimulation and lower Ca<sup>2+</sup> concentrations that reduce quantal content and therefore depression to examine quantal content at rest and during post-tetanic potentiation.

Many of our results concern changes in quantal content, the average number of quantal released by each presynaptic action potential. We use this term in the original sense of the number of electrophysiologically detectable quanta that make up the EPP. A semantic issue arises when one equates the quanta with synaptic vesicles and considers the possibility of empty vesicles. In this case the term “quantal content” is ambiguous; it could mean the number of quanta of neurotransmitter released or it could mean the total number of vesicles released. We will continue to use “quanta” and “quantal content” in the electrophysiological sense, and will use phrases like “number of vesicles released” when needed. This distinction is relevant to our results on facilitation because changes in quantal content are often associated with changes in paired pulse facilitation. The classic example is the association between quantal content and facilitation when release probability is manipulated by changing the extracellular Ca<sup>2+</sup>/Mg<sup>2+</sup> ratio (Mallart and Martin, 1968). We observed lower quantal content in VACHT-KD<sup>HOM</sup> animals without any change in facilitation. This suggests that quantal content is lower not because of reduced release probability, but rather a because of a smaller supply of quanta.

### Baseline quantal parameters under low-frequency stimulation

In vivo, vesicular ACh does not achieve thermodynamic equilibrium with cytoplasm ACh (Parsons, 2000). The specific molecular mechanisms by which quantal size may be regulated are largely unknown, but the activity of vesicular neurotransmitter transporter is an obvious candidate, and experimental evidence exists both for and against this possibility, as reviewed by Van der Kloot, (2003). Overexpression of VACHT caused increased ACh uptake by PC12 cell post-nuclear homogenates (Varoqui and Erickson, 1996) and larger spontaneous EPSCs in co-cultured *Xenopus* spinal neurons and myocytes (Song et al, 1997). In addition, increasing the concentration of ACh also increased its uptake into PC12 cell membranes (Varoqui and Erickson, 1996). Similar observations have been made for uptake of glutamate into synaptic vesicles from CNS neurons (Ishikawa et al., 2002; Wilson et al, 2005). All of these results are consistent with the idea that vesicle filling represents a dynamic steady-state between uptake and passive leak. Our present results provide further support for this model, as reduced VACHT expression reduced MEPP amplitude, although we cannot rule out the possibility of differences in post-synaptic sensitivity in the VACHT KD<sup>HOM</sup> mice. To overcome the possibility of changes in post-synaptic sensitivity, data on quantal content was obtained either by measuring EPP and MEPPs at the same synapse permitting calculation by the direct method or by the statistical methods of (Del-Castillo and Katz, 1954). In either case, results are independent of post-synaptic sensitivity.

The reduction of basal quantal content in VACHT KD<sup>HOM</sup> neuromuscular junctions was surprising because the low stimulation frequency used produces minimal synaptic rundown and vesicle recycling therefore is able to keep up with release. Moreover, previous experiments with FM1-43 indicated the quantity of recycling vesicles was normal in NMJs

from VAcHT KD<sup>HOM</sup> mice (Prado et al., 2006), and experiments measuring paired-pulse facilitation or initial EPP rundown during high-frequency trains revealed no evidence for changes in release probability. One possibility to explain these data is the presence of a population of synaptic vesicles that do not contain VAcHT and thus are unable to take up much acetylcholine. Cholinergic synaptic vesicles in the electric organ of *Torpedo* contain on average about four copies of VAcHT (Bahr and Parsons, 1986). Cholinergic vesicles in mammalian NMJs have about half the diameter (Volkhardt and Zimmermann, 1986) and therefore one-fourth the membrane surface area of *Torpedo* vesicles. The distribution in the number of copies of VAcHT per mammalian vesicle is unknown, but if the mean number is small it is expected that some vesicles will contain zero copies of VAcHT and that this fraction of “silent vesicles” will be higher in VAcHT KD<sup>HOM</sup> neuromuscular junctions.

Although vesicles without VAcHT may be poorly detected by electrophysiological recordings, much evidence suggests they will still recycle normally. Studies at the neuromuscular junction with the dye FM1-43 indicated that cholinergic synaptic vesicle recycling continued to occur in nerve terminals stimulated in the presence of vesamicol (Parsons et al., 1999). Similar results were obtained when choline uptake into the terminal was blocked by hemicholinium (Ceccarelli and Hurlbut, 1975). In hippocampus slices, blocking the vATPase reduced the amplitude and frequency of mEPSPs and mEPSCs, but did not alter vesicle recycling as recorded by FM dye detaining, leading to the conclusion that depleted or empty vesicles recycle normally (Zhou et al., 2000). Moreover, recent experiments using transgenic mice expressing synaptotagmin indicated continued strong exocytosis even as synaptic depression reached 100%. It was suggested that exocytosis without a post-synaptic potential reflects fusion of “empty” synaptic vesicles or other acidified membranous structures (Tabares et al., 2007). Together these results indicate that empty vesicles compete with normal vesicles for the exocytosis apparatus, and that in the VAcHT KD<sup>HOM</sup> mice an increase in vesicles without VAcHT reduces the apparent quantal content of EPPs and the frequency of MEPPs.

### Vesicle pools in the mouse neuromuscular junction

Many synapses contain multiple anatomically and functionally distinct pools of synaptic vesicles and multiple recycling pathways (Rizzoli and Betz, 2005). At the mouse neuromuscular junction, about 1% of vesicles reside in a rapidly releasable pool and are preferentially released by low-frequency stimulation or during the initial phase of high-frequency stimulation (Perissinotti et al., 2008; Zefirov et al., 2009). Release during prolonged high-frequency stimulation may be due to recruitment of vesicles from a reserve or due to rapid recycling of recently released vesicles. These two possibilities have been distinguished by combining post-synaptic recordings to measure released quanta with FM dye detaining to measure exocytosis of a previously labeled vesicle. Comparison of exocytosis by these two techniques at the mouse NMJ indicates preferential rapid recycling back to the readily releasable pool during tetanic stimulation (Perissinotti et al., 2008; Zefirov et al., 2009). Thus tetanic stimulation specifically increases the demand on refilling of synaptic vesicles, not only because more vesicles are released but also because they are replaced by rapid recycling.

### Role of VAcHT in expression of post-tetanic potentiation

Although a population of silent vesicles may explain the lower basal quantal content of EPPs and frequency of MEPPs in VAcHT KD<sup>HOM</sup> NMJs, it cannot explain the loss of post-tetanic potentiation because we followed the usual practice of expressing post-tetanic transmitter release (EPP amplitudes, or MEPP frequency) in proportion to control values measured at the same synapse before the conditioning train. Silent vesicles are thus factored out of this calculation. Rather, the data suggest that the level of VAcHT activity determines



the ability of the synapse to increase its output during potentiation. Possible mechanisms for the loss of potentiation in VACHT KD<sup>HOM</sup> mice include reduced final loading of synaptic vesicles (Naves and Van der Kloot, 2001) and longer vesicle refilling times expected if the average number of copies of VACHT per vesicle is reduced.

If VACHT KD<sup>HOM</sup> synapses show a loss of potentiation because they cannot keep up with the increased demands for vesicle refilling, one might expect a reduction in quantal size at the end of a tetanic stimulation. It was therefore surprising that we did not observe a reduction in the amplitudes of MEPPs after tetanic stimulation. It is generally assumed that MEPPs and evoked quanta come from the same vesicle pool, although in cultured hippocampal neurons there is evidence for and against a separate pool of spontaneously releasing vesicles that recycle separately from the evocable pool (Sara et al., 2005; Groemer and Klingauf, 2007; Fredj and Burrone, 2009). Previous studies showed vesamicol reduces post-tetanic potentiation without reducing quantal size (Maeno and Shibuya, 1988). Recently, evidence for exocytosis of empty vesicles at the neuromuscular junction has been presented after complete EPP rundown during high-frequency stimulation (Tabares et al., 2007). In this study the authors also did not observe a reduction in the size of asynchronously or spontaneously released quanta during or after the stimulus train, as may have been expected if vesicle recycling and refilling could not keep up with demand. These data indicate that lack of change in quantal size after tetanic stimulation cannot be taken as evidence for normal vesicle recycling and refilling.

In mice NMJs, mitochondria sequester Ca<sup>2+</sup> during high frequency stimulation and its release in the post-tetanic period correlates with enhanced transmitter release (García-Chacón et al., 2006). This behavior suggests a mechanism to activate transmitter release for post-tetanic potentiation. However, for calcium to increase release, recycling and refilling of the pool of vesicles involved in potentiation need to be efficient. Because vesicle loading is mediated by VACHT, refilling of rapidly recycling vesicles should be preferentially affected in VACHT KD<sup>HOM</sup> mice. Experiments with fluorescent dyes at the frog neuromuscular junction have indicated the existence of two pools of synaptic vesicles, a smaller capacity, readily releasable population that recycles rapidly, and a larger reserve population that is reluctantly releasable and recycles more slowly (Richards et al., 2000; Richards et al., 2003). Our data suggest that post-tetanic potentiation increases the fusion of vesicles that have rapidly recycled. When VACHT activity is reduced, some of these vesicles refill with ACh and some do not.

## Acknowledgments

We thank Dr. William Van der Kloot and Dr. Stanley M. Parsons for valuable comments on a draft of this paper. Supported by FAPEMIG (CBB APQ-4536-4.01/07 and PRONEX), NIH-Fogarty grant R21 TW007800-02, CIHR (MOP-89919, V.F.P. and M.A.M.P.), Heart and Stroke Foundation of Ontario (NA 6656, M.A.M.P. and V.F.P.), CNPq (Aging and Mental Health Programs, Universal 474445/2007-0), Instituto do Milenio Toxins/MCT

## References

- Bahr BA, Parsons SM. Demonstration of a receptor in Torpedo synaptic vesicles for the acetylcholine storage blocker L-trans-2-(4-phenyl[3,4-<sup>3</sup>H]-piperidino) cyclohexanol. *Proc Natl Acad Sci U S A*. 1986; 83:2267–2270. [PubMed: 3457385]
- Bain AI, Quastel DM. Multiplicative and additive Ca<sup>2+</sup>-dependent components of facilitation at mouse endplates. *J Physiol*. 1992; 455:383–405. [PubMed: 1484358]
- Barstad JA, Lilleheil G. Transversally cut diaphragm preparation from rat. An adjuvant tool in the study of the physiology and pharmacology of the myoneural junction. *Arch Int Pharmacodyn Ther*. 1968; 175:373–390. [PubMed: 5702955]

- de Castro BM, Jaeger XD, Martins-Silva C, Lima RDF, Amaral E, Menezes C, Lima P, Neves CML, Pires RG, Gould TW, Welch I, Kushmerick C, Guatimosim C, Izquierdo I, Cammarota M, Rylett RJ, Gomez MV, Caron MG, Oppenheim RW, Prado MAM, Prado VF. The vesicular acetylcholine transporter is required for neuromuscular development and function. *Mol Cell Biol.* 2009; 29:5238–5250. [PubMed: 19635813]
- Ceccarelli B, Hurlbut WP. The effects of prolonged repetitive stimulation in hemicholinium on the frog neuromuscular junction. *J Physiol.* 1975; 247:163–188. [PubMed: 1079538]
- Del-Castillo J, Katz B. Quantal components of the end-plate potential. *J Physiol.* 1954; 124:560–573. [PubMed: 13175199]
- Erickson JD, Varoqui H, Schäfer MK, Modi W, Diebler MF, Weihe E, Rand J, Eiden LE, Bonner TI, Usdin TB. Functional identification of a vesicular acetylcholine transporter and its expression from a “cholinergic” gene locus. *J Biol Chem.* 1994; 269:21929–21932. [PubMed: 8071310]
- Fisher SA, Fischer TM, Carew TJ. Multiple overlapping processes underlying short-term synaptic enhancement. *Trends Neurosci.* 1997; 20:170–177. [PubMed: 9106358]
- Fredj NB, Burrone J. A resting pool of vesicles is responsible for spontaneous vesicle fusion at the synapse. *Nat Neurosci.* 2009; 12:751–758. [PubMed: 19430474]
- Gage PW, Hubbard JI. An investigation of the post-tetanic potentiation of end-plate potentials at a mammalian neuromuscular junction. *J Physiol.* 1966; 184:353–375. [PubMed: 5921835]
- García-Chacón LE, Nguyen KT, David G, Barrett EF. Extrusion of  $\text{Ca}^{2+}$  from mouse motor terminal mitochondria via a  $\text{Na}^{+}$ - $\text{Ca}^{2+}$  exchanger increases post-tetanic evoked release. *J Physiol.* 2006; 574:663–675. [PubMed: 16613870]
- Groemer TW, Klingauf J. Synaptic vesicles recycling spontaneously and during activity belong to the same vesicle pool. *Nat Neurosci.* 2007; 10:145–147. [PubMed: 17220885]
- Ishikawa T, Sahara Y, Takahashi T. A single packet of transmitter does not saturate postsynaptic glutamate receptors. *Neuron.* 2002; 34:613–621. [PubMed: 12062044]
- Lara A, Damasceno DD, Pires R, Gros R, Gomes ER, Gavioli M, Lima RF, Guimarães D, Lima P, Bueno CR, Vasconcelos A, Roman-Campos D, Menezes CAS, Sirvente RA, Salemi VM, Mady C, Caron MG, Ferreira AJ, Brum PC, Resende RR, Cruz JS, Gomez MV, Prado VF, de Almeida AP, Prado MAM, Guatimosim S. Dysautonomia due to reduced cholinergic neurotransmission causes cardiac remodeling and heart failure. *Mol Cell Biol.* 2010 [Epub ahead of print].
- Magleby KL, Zengel JE. A quantitative description of stimulation-induced changes in transmitter release at the frog neuromuscular junction. *J Gen Physiol.* 1982; 80:613–638. [PubMed: 6128373]
- Mallart A, Martin AR. The relation between quantum content and facilitation at the neuromuscular junction of the frog. *J Physiol.* 1968; 196:593–604. [PubMed: 4298821]
- Martin AR. Quantal nature of synaptic transmission. *Physiol Rev.* 1966; 46:41–46.
- McLachlan EM, Martin AR. Non-linear summation of end-plate potentials in the frog and mouse. *J Physiol.* 1981; 311:307–324. [PubMed: 6267255]
- Naves LA, Van der Kloot W. Repetitive nerve stimulation decreases the acetylcholine content of quanta at the frog neuromuscular junction. *J Physiol.* 2001; 532:637–647. [PubMed: 11313435]
- Nussinovitch I, Rahamimoff R. Ionic basis of tetanic and post-tetanic potentiation at a mammalian neuromuscular junction. *J Physiol.* 1988; 396:435–455. [PubMed: 2457692]
- Parsons RL, Calupca MA, Merriam LA, Prior C. Empty synaptic vesicles recycle and undergo exocytosis at vesamicol-treated motor nerve terminals. *J Neurophysiol.* 1999; 81:2696–2700. [PubMed: 10368389]
- Parsons SM. Transport mechanisms in acetylcholine and monoamine storage. *FASEB J.* 2000; 14:2423–2434. [PubMed: 11099460]
- Perissinotti PP, Tropper BG, Uchitel OD. L-type calcium channels are involved in fast endocytosis at the mouse neuromuscular junction. *Eur J Neurosci.* 2008; 27:1333–1344. [PubMed: 18336569]
- Prado VF, Martins-Silva C, de Castro BM, Lima RF, Barros DM, Amaral E, Ramsey AJ, Sotnikova TD, Ramirez MR, Kim H-G, Rossato JI, Koenen J, Quan H, Cota VR, Moraes MFD, Gomez MV, Guatimosim C, Wetsel WC, Kushmerick C, Pereira GS, Gainetdinov RR, Izquierdo I, Caron MG, Prado MAM. Mice deficient for the vesicular acetylcholine transporter are myasthenic and have deficits in object and social recognition. *Neuron.* 2006; 51:601–612. [PubMed: 16950158]

- Prior C, Marshall IG, Parsons SM. The pharmacology of vesamicol: an inhibitor of the vesicular acetylcholine transporter. *Gen Pharmacol.* 1992; 23:1017–1022. [PubMed: 1487110]
- Richards DA, Guatimosim C, Betz WJ. Two endocytic recycling routes selectively fill two vesicle pools in frog motor nerve terminals. *Neuron.* 2000; 27:551–559. [PubMed: 11055437]
- Richards DA, Guatimosim C, Rizzoli SO, Betz WJ. Synaptic vesicle pools at the frog neuromuscular junction. *Neuron.* 2003; 39:529–541. [PubMed: 12895425]
- Rizzoli SO, Betz WJ. Synaptic vesicle pools. *Nat Rev Neurosci.* 2005; 6:57–69. [PubMed: 15611727]
- Roghani A, Feldman J, Kohan SA, Shirzadi A, Gundersen CB, Brecha N, Edwards RH. Molecular cloning of a putative vesicular transporter for acetylcholine. *Proc Natl Acad Sci U S A.* 1994; 91:10620–10624. [PubMed: 7938002]
- Sara Y, Virmani T, Deák F, Liu X, Kavalali ET. An isolated pool of vesicles recycles at rest and drives spontaneous neurotransmission. *Neuron.* 2005; 45:563–573. [PubMed: 15721242]
- Searl T, Prior C, Marshall IG. Acetylcholine recycling and release at rat motor nerve terminals studied using (–)-vesamicol and troxpyrrolium. *J Physiol.* 1991; 444:99–116. [PubMed: 1668355]
- Song H, Ming G, Fon E, Bellocchio E, Edwards RH, Poo M. Expression of a putative vesicular acetylcholine transporter facilitates quantal transmitter packaging. *Neuron.* 1997; 18:815–826. [PubMed: 9182805]
- Sudhof TC. The synaptic vesicle cycle. *Annu Rev Neurosci.* 2004; 27:509–547. [PubMed: 15217342]
- Tabares L, Ruiz R, Linares-Clemente P, Gaffield MA, de Toledo GA, Fernandez-Chacón R, Betz WJ. Monitoring synaptic function at the neuromuscular junction of a mouse expressing synaptopHluorin. *J Neurosci.* 2007; 27:5422–5430. [PubMed: 17507564]
- Van der Kloot W. Loading and recycling of synaptic vesicles in the Torpedo electric organ and the vertebrate neuromuscular junction. *Prog Neurobiol.* 2003; 71:269–303. [PubMed: 14698765]
- Varoqui H, Erickson JD. Active transport of acetylcholine by the human vesicular acetylcholine transporter. *J Biol Chem.* 1996; 271:27229–27232. [PubMed: 8910293]
- Volkandt W, Zimmermann H. Acetylcholine, ATP, and proteoglycan are common to synaptic vesicles isolated from the electric organs of electric eel and electric catfish as well as from rat diaphragm. *J Neurochem.* 1986; 47:1449–1462. [PubMed: 3760871]
- Wilson DF, Skirboll LR. Basis for posttetanic potentiation at the mammalian neuromuscular junction. *Am J Physiol.* 1974; 227:92–95. [PubMed: 4843361]
- Wilson NR, Kang J, Hueske EV, Leung T, Varoqui H, Murnick JG, Erickson JD, Liu G. Presynaptic regulation of quantal size by the vesicular glutamate transporter VGLUT1. *J Neurosci.* 2005; 25:6221–6234. [PubMed: 15987952]
- Zefirov AL, Zakharov AV, Mukhametzyanov RD, Petrov AM, Sitdikova GF. The vesicle cycle in motor nerve endings of the mouse diaphragm. *Neurosci Behav Physiol.* 2009; 39:245–252. [PubMed: 19234803]
- Zengel JE, Magleby KL, Horn JP, McAfee DA, Yarowsky PJ. Facilitation, augmentation, and potentiation of synaptic transmission at the superior cervical ganglion of the rabbit. *J Gen Physiol.* 1980; 76:213–231. [PubMed: 6251156]
- Zengel JE, Sosa MA. Changes in MEPP frequency during depression of evoked release at the frog neuromuscular junction. *J Physiol.* 1994; 477(Pt 2):267–277. [PubMed: 7932218]
- Zhou Q, Petersen CC, Nicoll RA. Effects of reduced vesicular filling on synaptic transmission in rat hippocampal neurones. *J Physiol.* 2000; 525(Pt 1):195–206. [PubMed: 10811737]
- Zucker RS. Short-term synaptic plasticity. *Annu Rev Neurosci.* 1989; 12:13–31. [PubMed: 2648947]
- Zucker RS, Regehr WG. Short-term synaptic plasticity. *Annu Rev Physiol.* 2002; 64:355–405. [PubMed: 11826273]

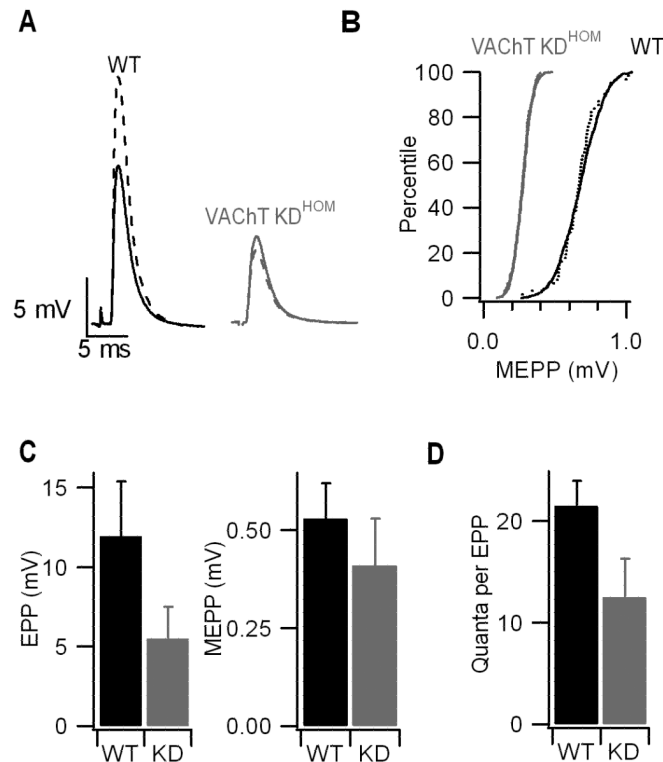


**Fig 1. Reduced quantal content in VACHT KD<sup>HOM</sup> neuromuscular junctions**

A. Representative end-plate potentials from a wild-type and an age-matched VACHT KD<sup>HOM</sup> end plate. Solid lines are the uncorrected recordings, broken lines are corrected for resting potential and non-linear summation. B. Amplitude distribution of MEPPs obtained from the same endplates used for Panel A. Points are individual MEPP amplitudes. Smooth lines are Gaussian distributions with mean and variance matched to the data. C. Average values of end-plate potentials and MEPP amplitude (WT) and VACHT KD<sup>HOM</sup> (KD). D. Quantal content, calculated by the direct method for each synapse.  $[Ca^{2+}] = 1.2$  mM.  $[Mg^{2+}] = 1.3$  mM. Error bars in C and D are 95% confidence limits. Differences are significant with  $P < 0.05$ .

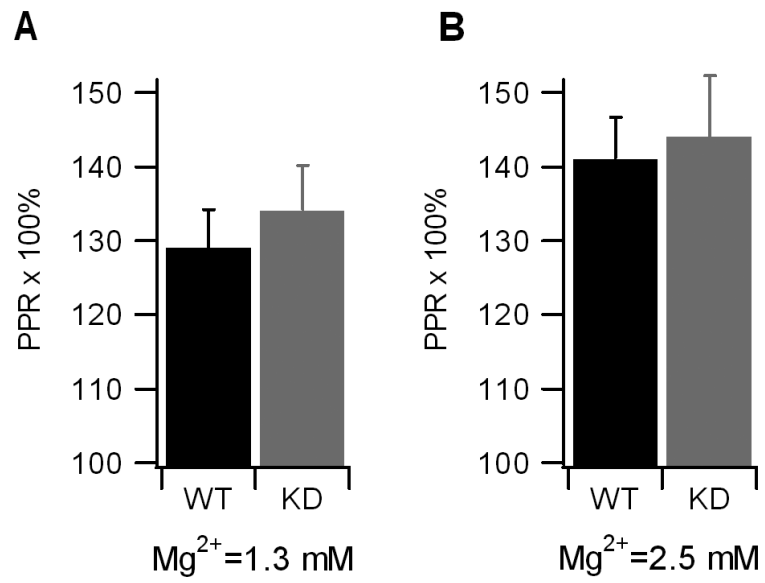


**Fig 2.** Paired pulse facilitation. Paired-pulse interval was 10 ms. WT: wild-type. KD: VAcHT KD<sup>HOM</sup>. [Ca<sup>2+</sup>]=1.2 mM. [Mg<sup>2+</sup>] as indicated. Error bars are 95% confidence intervals. Differences are not statistically significantly different.

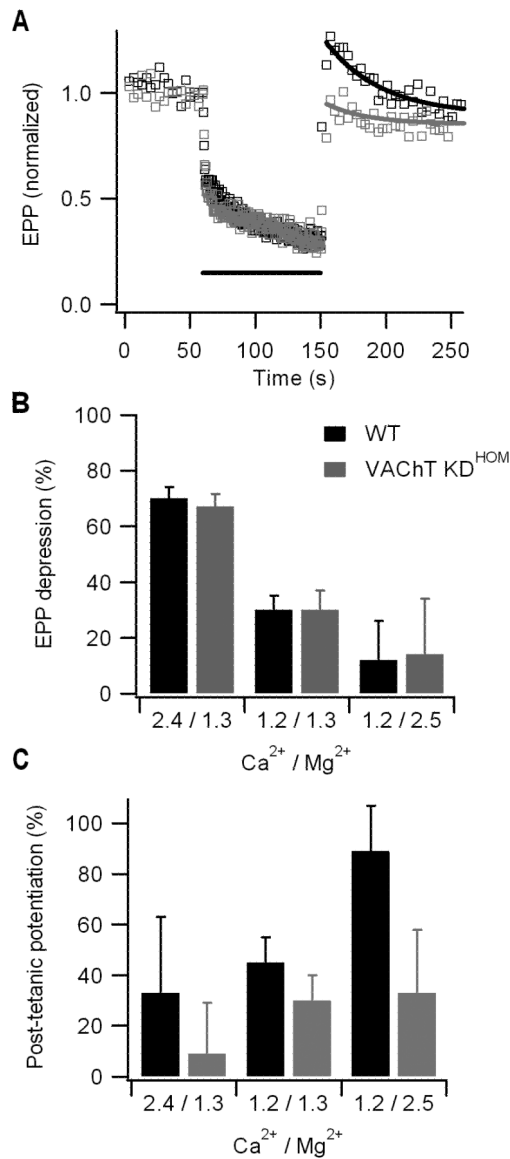


### Fig 3. Post-tetanic potentiation of EPP amplitude

A. EPP amplitude before, during, and after 30 Hz stimulation, indicated by the black bar. Initial stimulation frequency was 0.3 Hz. EPP amplitudes were normalized to the last 20 EPPs prior to the onset of high-frequency stimulation. For clarity, only every tenth EPP is shown during the high frequency stimulation. Solid lines are exponential fits to EPP amplitude during potentiation.  $[Ca^{2+}] = 2.4$  mM.  $[Mg^{2+}] = 1.3$  mM. B. Degree of depression at the end of high-frequency stimulation for three conditions of  $Ca^{2+}/Mg^{2+}$ . C. Amount of post-tetanic potentiation (amplitude of exponential component shown in A) for the three conditions in shown in part B. Error bars are 95% confidence intervals. Differences are significant with  $P < 0.05$ .

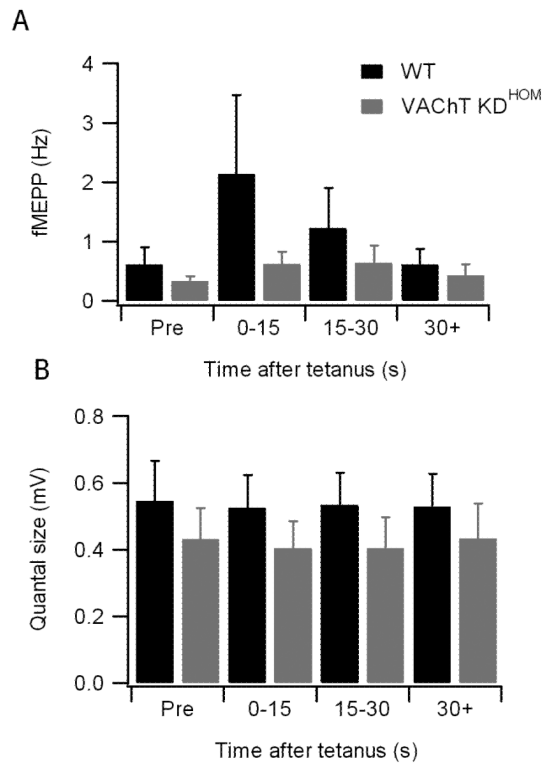


**Fig 4. Post-tetanic potentiation of MEPP frequency**

A. MEPP amplitudes prior to, and during three time bins after high-frequency stimulation.

B. MEPP frequency before and after tetanic stimulation. Error bars are 95% confidence intervals. Differences are significant with  $p < 0.05$ .

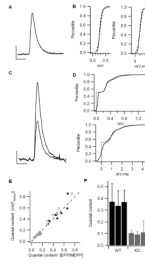


**Fig 5. Quantal composition of EPPs in 0.6 mM Ca<sup>2+</sup> / 7 mM Mg<sup>2+</sup>**

A-D MEPPs and EPPs recorded from a representative WT synapse. A. Average MEPP waveform. Scale bars are 0.1 mV and 5 ms. B. Distributions of MEPP amplitudes and time integrals. Solid lines are data, broken lines are Gaussian distributions with mean and variance matched to the data. C. Average presumed unquantal and diquantal EPP waveforms from the same synapse as above. D. Distributions of EPP amplitudes and areas. Solid lines are data. Broken lines are simulations as described in text. E. Summary data for WT (black) and VAcHT KD<sup>HOM</sup> (gray) synapses. At each synapse, quantal content was measured as  $-\ln(F_{\text{Failure}})$  and by the direct method (EPP/MEPP). Open symbols used EPP and MEPP amplitudes whereas filled symbols used areas for the direct method calculations. F. Summary of quantal content estimates using the three methods (from left to right,  $-\ln(F_{\text{Failure}})$ , direct method based on EPP and MEPP amplitudes, direct method based on EPP and MEPP areas). Error bars are 95% confidence limits. Difference between WT and VAcHT KD was significant ( $P < 0.05$ ).